A New Perspective and Explanation to the Formation of Plasmaspheric Shoulder Structure

Hua Zhang [1]   Guangshai Peng[1]   Chao Shen [2]

[1]Institute of Space Weather, Nanjing University of Information Science & Technology, Nanjing, China.

[2]Harbin Institute of Technology, Shen Zhen, China.

Correspondence to: Hua Zhang (289534957@qq.com)

Abstract

Over the hours of 5-9 UT on June 8 2001, the extreme ultraviolet (EUV) instrument onboard IMAGE satellite observed a Shoulder-like formation in the morning sector and a Plume-like structure straddling in the between noon and dusk region. The plasmapause formation is simulated using the Test Particle Model (TPM), based on drift motion, which reproduces various plasmapause structures and evolution of the Shoulder feature. The analysis indicates that the Shoulder is created by sharp reduction and spatial nonuniform of a dawn-dusk convection electric field intensity. Combined action of the plasmaspheric rotation rate speeding up with L-shell and plasma flux doing radial outflow in the predawn sector, results in an asymmetric bulge rotating eastward to reproduce the Shoulder structure. The Shoulder structure rotates sunward and develops to the single or double Plume structure during an active times.

Keywords: plasmapause; shoulder-like; plume-like;IMAGE/EUV

1. Introduction

The plasmasphere is important region in the inner magnetosphere, surrounding the Earth and extending to 5 Earth radii(Re), which contains dense(10-10000 cm^{-3}) and cold plasma (below 1ev). The plasmapause formed by a superposition of corotation and convection electric field in the inner magnetosphere (Nishida,1966; Chen and Wolf, 1972). The formation and size of plasmapause varies with geomagnetic activity level. Generally, as the disturbance level increasing, the plasmapause position closer

to the Earth and of shape deviate from circle in the equatorial plane (Grebowsky, 1970). Atypical plasmapause structures, such as 'bulge' and Plume occur often in both whistler and in-situ data (Carpenter and Anderson,1992). There are many theoretical researches study to explanation of the formation of Plume (Grebowsky,1970; Pierrard and Lemaire, 2004; Zhang et al., 2013), and Pierrard and Cabrera (2006) firstly simulated a double-Plumes , but not explained origin of second-Plume.

The EUV instrument onboard IMAGE satellite has launched in March, 2000, which provided a global perspective to the plasmasphere, such as Plume, Finger, Notch and Shoulder, and so on, some of plasmaspheric structures observed by EUV (Sandel et al., 2001). One of plasmaspheric structures, Shoulder, has less study in the previous papers than Plume. But, the Shoulder may play important role on a loss mechanism for the ring current (Burch et al., 2001). So, it is important to study the formation mechanism of Shoulder.

At present, there are no convincing explanations for dynamic formation of Shoulder. Goldstein et al.(2002) firstly proposed an explanation, based on the Magnetospheric Specification Model(MCM) simulation output, for the formation of the Shoulder. They presented that the Shoulder is created by sudden decrease of dusk-dawn electric field. As interplanetary magnetic field (IMF) turns northward from southward, trigger antisunward flow of plasma in predawn sector, to produce an asymmetric bulge called Shoulder. Later, based on physical mechanism of interchange instability and a Kp-dependent E5D electric field model, Pierrard and Lemaire (2004) suggested that the Shoulder is not the result of radial outflow of plasma, same as the presentation of Goldstein et al. (2002) , but is inward plasma drift in post-midnight sector.

Then, scarce papers about dynamical formation of the Shoulder are delivered than of Plume. In this paper, we used TPM to simulate dynamical formation of the Shoulder, using Weimer's statistical E-field (Weimer, 2001; Zhang et al., 2012), which is both spatially nonuniform and dynamically responsive to change geomagnetic and solar wind conditions. To drive the TPM model, several inputs are used: Dst; solar wind (SW) and interplanetary magnetic field (IMF) data sets. The

59 authors make attempt to a new convincing explanation for formation of the

60 Shoulder-like structure, different from the previous explanations.

2. Shoulder Observation

62
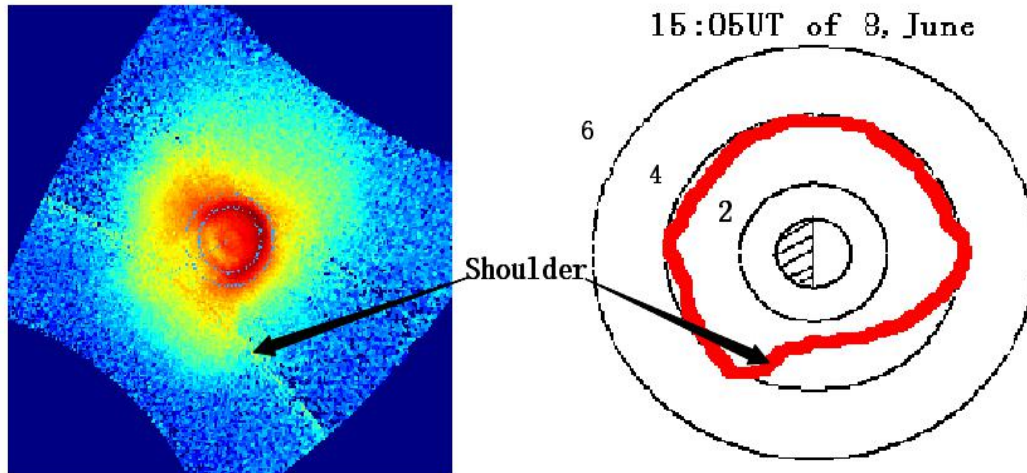
Figure1. Snapshot of plasmasphere(left panel) by EUV instrument, at 15:05 UT of 8 June 2001, Sunlight is incident from the upper right. Earth is in the center of panels and Shoulder is observed and labeled in the snapshot. Right panel is plasmapause of that extracted from left plasmapheric image.

The Figure 1 illustrates the Shoulder-like structure, a sharp radial plasmaspheric structure about 1 RE radial extension, in the post-midnight sector, which was viewed by EUV imager onboard IMAGE satellite at 15.05 UT of 8 June 2001. The right panel illustrates the plasmapause extracted from the left panel in the Figure1. The outer boundary of plasmasphere is assumed to be 40% of maximum brightness of 30.4nm He^+ emission, where the intensity is the logarithm of the luminosity (Pierrard and Cabrera, 2006). Then, the Shoulder-like is labeled and marked by arrows in the plot. Comparison sequential observations with the simulation pictures, show that the Shoulder structure keeping and corotating with the main plasmaspheric body can be seen in Figure 3, and is discussed in the next section. That is mean the outer edge of the Shoulder corotates faster than the inner edge in development phase (Goldstein et al., 2002). Then, the Shoulder moves eastward to afternoon sector and evolves into the Plume-like structure. Over the next hours, the outer body of Plume flows sunward from noon sector, resulting in the Plume thinned out and disappeared (can see the

81 simulation of Figure 3). In the next section, we take the case of 8 June 2001

82 observation as an example, to discuss the simulation of the Shoulder and the Plume

83 evolution based on the TPM method.

3. Simulation

85 In region of plasmasphere occupied, charged particles are cold plasma (e.g. energy of

86 particles is <1 eV). So, we can assume that plasma elements have only $\boldsymbol{E} \times \boldsymbol{B}/B^2$ drift

87 motions (Li and Xu, 2005; Lejosne and Mozer, 2016). Here, the electric field intensity

88 of E-model is superposition of convection and corotation electric field. Electric field

89 plays a key role on plasma drift motion and the formation of plasmasphere (Pierrard et

90 al., 2008). In the present paper, the Weimer's electric field (Weimer, 2001) is mapped

91 into the magnetosphere along magnetic lines to model the magnetospheric convection

92 electric field (Zhang et al., 2012), and T96 magnetic field to model the background

93 magnetic field.

94 In the simulation, the calculation regions is radial range of 2-7 Re and azimuthal

95 span 0-359°. Dispersion by iso-spacing grids that correspond to the radial and

96 azimuthal steps are equal to 0.1Re and 1° respectively, in the magnetic equatorial

97 plane. Ten particles are placed into each grid, so particle density is proportional to

98 L^{-1} which is not consistent with the actual density in a saturation state (close to true

99 density presumably is proportional to L^{-4}), but is adequate to study the evolution of

100 plasmaspheric morphology using a skeleton map of particles during a substorm period.

101 The TMP runs 3 days under the low activity condition to obtain the boundary conditions for

102 the simulation.
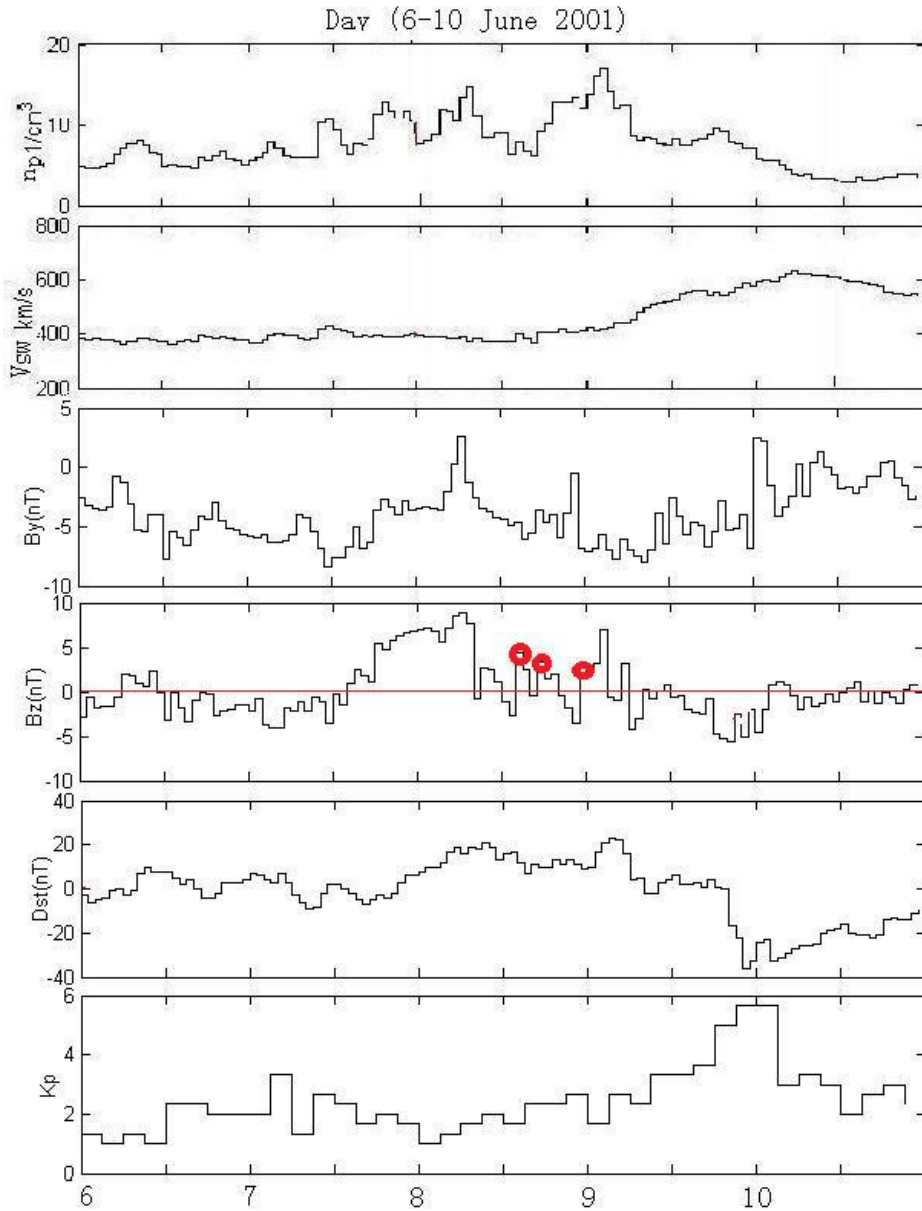
Figure 2. Input parameters of TPM model, the variation of the By and Bz component of the IMF, the Dst index and Kp index, on 6 -10 June 2001, is a typical substorm case.

The paper presents the case of 8-9 June 2001, to study the evolution of the shoulder and propose a hypothetical explanation produced by TPM simulation. During the geomagnetic substorm, all of the TPM inputs are available. IMF and Solar Wind data are available in ACE satellite data center, and Dst index can see in World Data center for Geomagnetism, Kyoto. Fig.2 shows the By, Bz components of the IMF, the Dst index and the geomagnetic activity index Kp, observed over 6 to 10 June 2001. This is a typical substorm case that Kp index gradually increases up to 5+ and then decreases. The TPM runs with 3-minute

time resolution from 6 June at 00:00 UT to 10 June at 12:00 UT. The results of simulation are showed in Fig.3, whose corresponding times are labeled on the title of each panel. The simulation plasmapauses is a skeleton which consists of continuous particles distribution. Comparison of TPM simulation (black body) and EUV observation (red line) in Fig.3, the simulated plasmapause positions correspond generally rather favorable with the EUV observations. The results of EUV observation show that the plasmapause is seldom smooth or irregular, due to the fluctuations in plasmapause region cause by successive particles injection during a disturbance period (Goldstein et al., 2002; Gallagher et al., 2005), in agreement with previous whistler observations (Carpenter and Anderson,1992). Contrary, The simulation of plasmapauses by TPM is better smooth. So, observations and simulations are not identical, due to deviation in the extraction of the boundary from EUV image and optical contamination of the image (Sandel et al., 2001; Zhang et al., 2013) and the limitation in the TPM model and the unrealistic Weimer electric field model. .

129
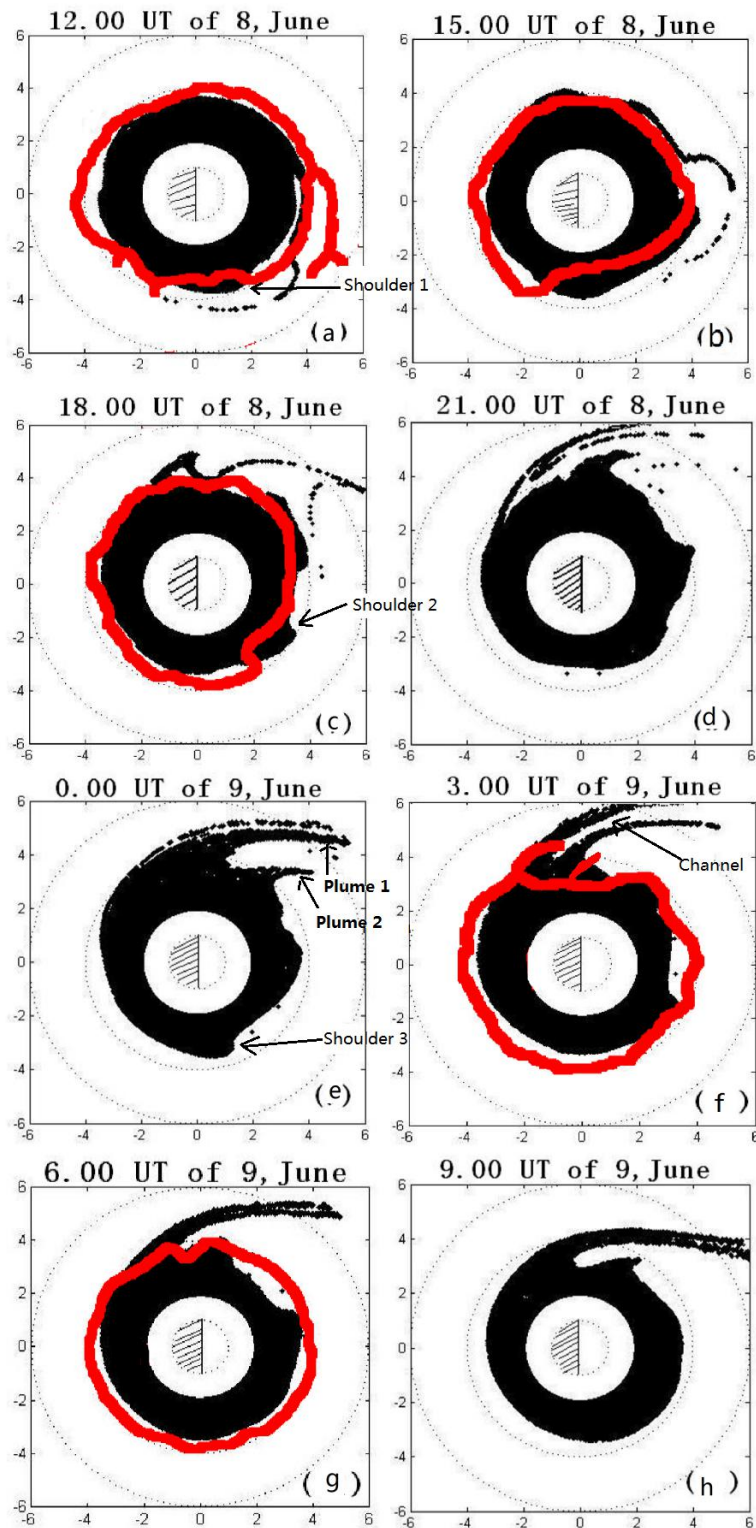
Figure 3. The simulation of plasmaspheric morphology compare with EUV/IMAGE observation in the geomagnetic equatorial plane on 8 - 9 June 2001. The red irregular curves indicate the plasmapause observation by EUV/IMAGE. Black contours are the plasmasphere simulated by TPM model. White contours are main plasmasphere (located at 1-2 Re region).The dotted circles on the panels correspond

134   to L=1, 2, 4 and 6.

135   Panels of Fig.3(a) - (h) illustrate the plasmasphere obtained on the interval of from

136   8 June at 12:00 UT to 9 June at 09:00 UT 2001, and every three hours output a

137   snapshot. The results of the simulation show that the evolution and development of

138   the features of the plasmapause, like Shoulders and Plumes. One can see that the

139   plasmapause is closer to the Earth in the predawn sector. The reason is the increase of

140   rotation velocity resulting in plasmapause of inward flow in the predawn sector

141   (Pierrard and Cabrera, 2006; Verbanac et al., 2018). At 15.05 UT of 8 June, the TMP

142   simulation captures a infant Shoulder-like structure in panel Fig.3 (b), and then

143   corotates with the plasmasphere body moved eastward and further reproduces a

144   mature Shoulder formation in Fig.3(c). The overall agreement between TPM

145   simulation and EUV observed is quite well, but the TPM Shoulder is located ~1.5

146   hours earlier in magnetic local time (MLT) that probably originated from the

147   convection electric field model (Goldstein et al., 2002; Pierrard and Cabrera, 2005;

148   Zhang et al., 2013).

149   The EUV observation illustrated in Fig.3 (f) shows that a Plume is indeed observed

150   in the afternoon or dusk sector. The results of the simulation also reproduce the

151   formation and the evolution of the Plumes,which derives from the Shoulder structure

152   in this case, illustrated in panels of Fig.3 (d)-(f). The simulation show that the

153   Shoulders generate in the post-midnight sector (Verbanac et al., 2018), and then

154   rotates eastward around the Earth to the afternoon sector (Goldstein et al., 2002).

155   When the level of geomagnetic activity increase, the plasma element in the Shoulder

156   around the outer plasmasphere would convection outward and then into the dayside

157   magnetopause (Li and Xu, 2005; Pierrard et al., 2008), and produce the plasmaspheric

158   Plume structure. The Shoulder1 firstly arises on Fig.3(a) in the morning sector (at 12

159   UT, 8 June 2001), and then corotates with the main body of the plasmasphere to the

160   afternoon sector on Fig.3(c)(at 18 UT, 8 June 2001). During this period, Kp index

161   increases to 3+ from 1 (see in Fig.2), and magnetosphere convection slightly enhance

162   that triggers plasma elements in the Shoulder1 doing sunward convection, then

163   produces the Plume1 at 21 UT on 8 June 2001 (see in Fig.3(d)). The mature

164   Shoulder2, illustrated in Fig.3(b), corotates eastward with the Earth to the

165   afternoon-dusk sector. During period of 0-3 UT on June 9, Kp index gradually

166   increases up to 5+, indicating that magnetospheric convection is enhanced and the

167   convective electric field increases. The infantile Plume2, illustrated in the panel of

168   Fig.3(e), derives from outflow of plasma elements in the Shoulder2, and evolves into

169   the mature Plume2 in Fig.3(f). Later, the double-plumes formation that is extension

170   from the plasmapause to the magnetosphere, presented in the simulation results in

171   panels of Figs.3 (e)-(f).

172   The cavity in between the double Plumes, or between Plumes and the main body

173   of plasmasphere, may be responsible for the formation of Channel and Notch

174   structures (Gallagher et al., 2005). The base and the westward edge of the Plume is

175   connected with the main body of plasmasphere. And there is a cavity topology, a

176   low-density region, between the tail structure of the plasmasphere and the main body

177   of plasmasphere. That is the channel structure of the plasmasphere. The Plume

178   corotates with the Earth to become thinner, and disappear finally (Li and Xu, 2005).

179   The results of simulation reproduces the Channel structure in Fig.3(f). Gallagher et al.

180   (2005) proposes that Notches and Channels share same origin, which derive from a

181   low-density cavity in the dusk region during recovery at the base of the plasmaspheric

182   Plume. The absence of Notch structure in this simulation event, due to the fact that the

183   potential structure not cause the inward flow of plasma in the afternoon sector, and the

184   low disturbance time is maintaining for not long enough.

185   By contrastive analysis on between Fig.2 and Fig.3, the formation of the

186   Shoulder is produced during the intensity of the convection electric field sudden

187   decrease (Goldstein et al., 2002; Pierrard and Lemaire, 2004), when IMF sudden turns

188   northward from southward. There are three Shoulders reproduced during this

189   substorm period, depicted in panels of Fig.3 (b)-(g). The time of the Shoulder

190   appearance are labeled by three red circles in Fig.2, at 14:00 UT, 17:00 UT, 23:00 UT

191   on 8 June respectively. At moment, the Bz component of the IMF turns northward.

192   But, not all of the times of the Bz component of the IMF turns northward, could

193   produce the Shoulder structure. One can see that no shoulders reproduced in the

194   results of the simulation, at 02:00 UT, 05:00 UT, and 08:00 UT on 9 June 2001
195   respectively. The Bz value of southward component must less than previous 24-hours
196   mean value. The intensity of the convection electric field is greater than previous
197   24-hours level. So the last closed equipotential line (LCE) would closer to the Earth
198   and results in plasmapause of inward flow in the predawn sector (Zhang et al., 2013).

199   4. **Discussion**

200   The physical explanation of Shoulder formation is not yet understood. In present
201   section, we use the case of Figure 1 as an example to investigate the physical
202   mechanism of Shoulder formation based on the TPM model. Fourteen test particles
203   are placed in the range of $2.5 \leq L \leq 3.8$, initial position locate at 12:00 MLT, space step
204   takes 0.1Re, and then trace these particles motion. Outputs are the trajectory (see in
205   Fig.4(a)) and the rotation rate (see in Fig.4(b)) of these test particles corresponding to
206   both given magnetic local time and universal time illustrated in the bottom of Fig.4.
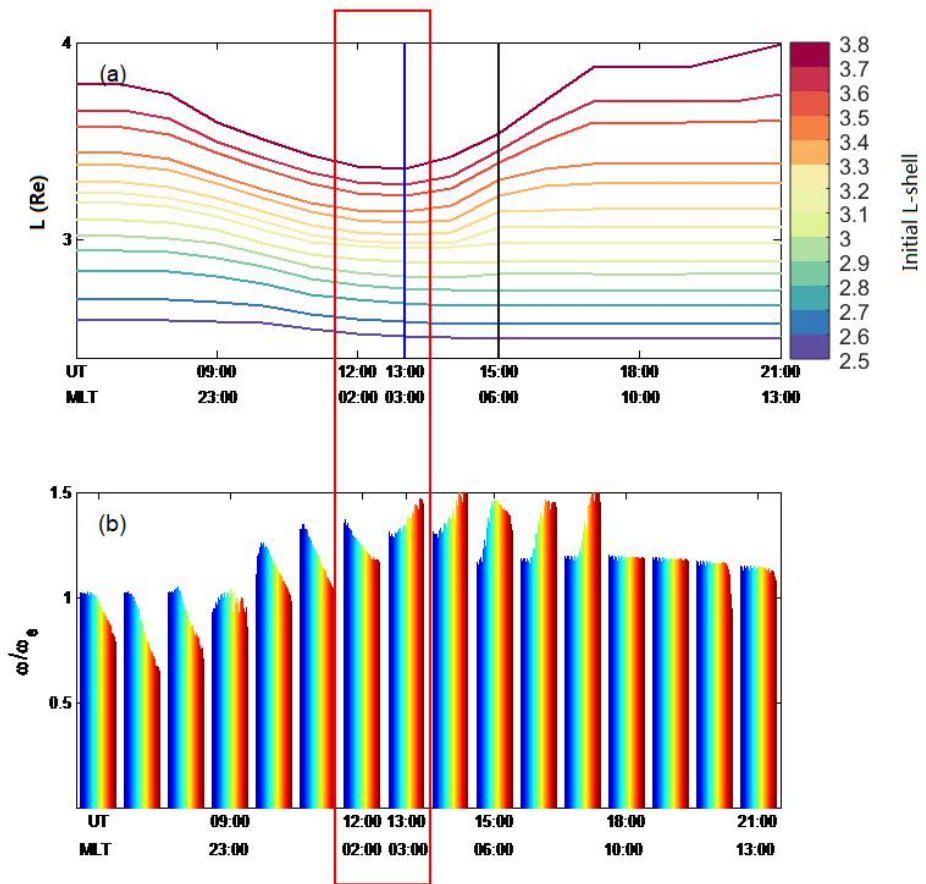
Figure 4. The trajectory (upper plot) and the rotation rate (bottom plot) of 14 test particles corresponding to both UT (time -dependent) and MLT (location-dependent) during a substorm. The legend indicates fourteen test particles of various initial L-shell. The day is 8 June 2001.

The top panel shows that the outer part of plasmasphere (L>3.3 Re) drift inward in the before 02:00MLT sector, and move outward (could reach up to 3.9 Re position) in the predawn sector (after 03:00MLT sector) (Verbanac et al., 2018). The radial motion of inner plasmasphere (L<3.3) is negligible.The shoulder forming across a at 03:00-06:00 MLT region (between blue vertical line and black vertical line in Figure 4(a)). The outermost particle move outward 0.7 Re, and the fourth particle move outward 0.45 Re, from 03:00 MLT to 08:00 MLT. So, the Shoulder has a sharp eastern edge about 0.2Re~0.3Re in radial extension and across a narrow 3-5 hours MLT region. Goldstein et al.(2002) proposed the shoulder formation by an outward radial

220 motion of plasma in a narrow range and in the morning sector. The conclusions of

221 Goldstein (2002) and Verbanac (2018) verify the simulation of this paper.

222   The lower panel shows the corotational angular velocity of test particles in the

223 range of 2.5 < L< 4.0. The simulation results suggest that plasma element in

224 plasmasphere region rotation speed varies significantly with radial distance (Galvan,

225 2010). The inner part of plasmasphere rotates faster than its outer part in before 02:00

226 MLT sector, vice versa in a range of in the 03:00-08:00 MLT sector [Lejosne and

227 Mozer, 2016]. The previous researchers analyzed the EUV observation and proposed

228 the Shoulder structure has MLT sharpening in the angular direction. It indicates that

229 the outer edge of the Shoulder rotates faster than the inner edge, resulting in

230 steepening of the MLT-profile of the Shoulder (Goldstein et al., 2002). The lower

231 panel shows, with the increase of L, the rotation rate of the plasmasphere tends to

232 slightly decrease on the dusk side and obviously increase on the dawn side.

233   Fig. 4 indicates, in the region of 21:00 - 23:00:00 MLT, that the rotation rate is

234 about corotation in the inner plasmasphere (L<3), but is the interval of 70% - 90% of

235 corotation in the outer plasmasphere (L>3). The rotational value decreases with the

236 increase of L [Galvan et al., 2010]. Gallagher et al. (2005) investigates the drift rate of

237 notches in the geomagnetic quite phase, and the results show that the average rotation

238 rate of plasmasphere is about 90% of the corotational rate, in agreement with the

239 results of Lejosne and Mozer (2016). When the plasma elements rotate to the region

240 of 23:00 - 02:00 MLT, rotation rate in the outer plasmasphere reaches to ~ 130% of

241 corotation, and in the inner plasmasphere is also close to the corotation rate. The

242 results show that the rotation rate of plasmasphere is overall increasing in the region.

243 In addition, the plasma elements in the outer plasmasphere rotate faster than the inner

244 plasmasphere in this region. The Fig.4(b) shows that rotation rate in the outer

245 plasmasphere highly reaches to ~ 140% of corotation, and rotation rate in the inner

246 plasmasphere is close to 110% of corotation. So, we propose that the physical

247 mechanism of the shoulder formation is plasma extrusion of outer plasmasphere in the

248 predawn sector, due to outer plasmasphere both drifts radial outward and rotates faster.

249 In present paper, the results show that the rotation rates of simulation are higher than

250   the observations, and not consistence with Huang et al. (2011) and Galvan et al.

251   (2010). The first reason is that this is a substorm case, so the convection of

252   magnetosphere is greater than the previous study articles of the geomagnetic quiet

253   case. (Galvan et al., 2010; Huang et al., 2011 ; Verbanac et al., 2018). And the second

254   reason is that the Weimer electric field model is larger in practice, which results in a

255   larger total electric field value in calculation (Goldstein et al., 2002; Pierrard et al.,

256   2008).

257   The dawn-dusk asymmetry of convective electric field is caused by the terminal

258   conductivity gradient of the ionosphere. The subrotation of the ionosphere drives the

259   subrotation of the plasmasphere, and the plasmaspheric drift is correlated with the

260   phase of geomagnetic storm (Burch et al., 2004). The convection electric field of

261   Weimer (2001) is obvious dawn-dusk asymmetry, that causes a smaller increase on

262   the dawnside and a lager decrease on the duskside, indicating that the subrotational

263   effect of the plasmasphere is modulated by field-aligned current changes and

264   conductance variations (Liemohn et al., 2004). The asymmetry of potential pattern

265   causes the sunward convection in the magnetospheric night-side to be larger than that

266   in the morning side, resulting in the subcorotational flow in the dark side. (Gallagher

267   et al., 2005).

268

5.   Conclusion

270   In this paper, we have simulated the case of substorm on 8 June 2001 to investigate

271   the physical mechanism of the Shoulder formation based on TPM model that utilizes

272   Weimer's electric field and the drift motion theory. We use the E-model and the

273   B-model are qusi-static background field and global averages. So, the results of

274   simulation have some deviations with EUV observation. But, we have satisfactorily

275   reproduced the evolution and development of the features of the plasmapause, like the

276   Shoulders and Plumes. And then, the physical mechanism of the Shoulder formation

277   has been investigated.

278   The formation of Shoulder is association with IMF northward turning in the

predawn sector. And the physical mechanism of Shoulder formation is the result of plasma extrusion in the predawn sector, caused by outer plasmasphere drifts radial outward and rotates faster. Reversal of corotation rate with L-shell in post-midnight sector compares with corotation rate in midnight sector. So, the shoulder forming across a at 03:00-06:00 MLT region.

The formation and evolution of Plume and Channel have also been reproduce in this case. One can see single or double Plumes appear in the dusk or afternoon sector, and then become thinner with time, finally disappear.

At this model, we not consider the refilling process of ionosphere. In the future work, the refilling process should be considered, expect to obtain more perfect results comparing with EUV observations. And also, the physical mechanisms of plasmaspheric features observed by EUV/IMAGE, like Notch or Channel, also are to investigate by TPM model in future work underway.

Author contributions: Zhang H. conceptualized the project and wrote the original draft of the paper. Peng G. S. modified the Figures and coded Fortran program. Shen C. supervised the project, and reviewed and edited the paper.

Acknowledgment: The author thanks the professor D. R. Weimer, who provided the code of Weimer's electric field model and ACE satellite data center and Word Data center for Geomagnetism, Kyoto provided observation data. The dataset of EUV/IMAGE could download from website http://euv.lpl.arizona.edu/euv.

References

Burch, J. L., Mende, S. B., Mitchell, D. G., Moore, T. E. , Pollock, C. J., Reinisch, B. W., Sandel, B. R., Fuselier, S. A. , and Gallagher D. L.: Views of Earth's magnetosphere with the IMAGE satellite, Science, 291, 691-624, doi: 10.1126/science.291.5504.619, 2001.

Carpenter, D. L. and Anderson, R. R.: An ISEE/Whistler model of equatorial electron density in the magnetosphere, J. Geophys. Res., 97, 1097-1108, doi:10.1029/91JA015481992, 1992.

309   Chen, A. J. and Wolf, R.A. : Effects on the plasmasphere of a time-varying convection

310   electric field, Planet. Space Sci., 20, 483-509, doi: 10.1016/0032-0633(72)90080-3,

311   1972.

312   Gallagher, D. L., Adrian, M. L. and Liemohn, M. W.: Origin and evolution of deep

313   plasmaspheric notches, J. Geophys. Res., 110, A09201, doi:10.1029/2004JA010906,

314   2005.

315   Galvan, D. A., Moldwin, M. B., Sandel, B. R., and Crowley, G. : On the cause of

316   plasmaspheric rotation variability: IMAGE EUV observation, J. Geophys. Res., 115,

317   A01214, doi:10.1029/ 2009JA014321, 2010.

318   Goldstein, J., Spiro,R. W., Reiff, P. H., Wolf, R. A., Sandel, B. R., Freeman, J. W., and

319   Lambour, R. L.: IMF-driven overshielding electric field and the origin of the

320   plasmaspheric shoulder of May 24, 2000, Geophys. Res. Lett., 29(16), 1819,

321   doi:10.1029/2001GL014534, 2002.

322   Grebowsky, J. M.: Model study of plasmapause motion, J. Geophys. Res., 75,

323   4329-4333, doi:10.1029/JA075i022p04329, 1970.

324   Huang Y., Xu, R. L., Shen, C., and Zhao H.: Rotation of the Earth's plasmasphere at

325   different radial distances, Adv. Space. Res., 48, 1167-1171, doi:

326   10.1016/j.asr.2011.05.028, 2011.

327   Lejosne, S., and Mozer, F. S. : Van Allen Probe measurements of the electric drift

328    $E{\times}B$/B^2 at Arecibo's L=1.4 field line coordinate, Geophys. Res. Lett., 43, 6768-6774,

329   doi: 10.1002/2016GL069875, 2016.

330   Li, L., and Xu, R. L.: Model of the evolution of the plasmasphere during a

331   geomagnetic storm, Adv. Space. Res., 36, 1895-1899. doi: 10.1016/j.asr.2003.10.057,

332   2005.

333   Nishida A.: Formation of plasmapause, or magnetospheric plasma knee, by the

334   combined action of magnetospheric convection and plasma escape from the tail, J.

335   Geophys. Res., 71, 5669-5679, doi:10.1029/JZ071i023p05669, 1966.

336   Pierrard V., and Lemaire, J. F.: Development of shoulders and plumes in the frame of

337   the interchange instability mechanism for plamapause formation, Geophys. Res. Lett.,

338   31, L05809, doi:10.1029/2003GL018919, 2004.

339   Pierrard, V., and Cabrera, J.: Comparisons between EUV/IMAGE observations and

340   numerical simulations of the plasmapause formation, Annales Geophysicae, 23,

341   2635-2646, doi:10.5194/angeo-23-2635-2005, 2005.

342   Pierrard, V., and Cabrera, J.: Dynamical simulations of plasmapause deformations,

343   Space.Sci.Res, 122, 119-126, doi: 10.1007/s11214-006-5670-3, 2006.

344   Pierrard, V., Khazanov, G. V., Cebrera, J., and Lemaire, J.: Influence of the convection

345   electric field models on predicted plasmapause positions during magnetic storms. J.

346   Geophys. Res. 113, A08212, doi:10.1029/2007JA012612, 2008.

347   Sandel, B. R., King, R. A., Forrester, W. T., Gallagher, D. L., Broadfoot, A. L., and

348   Curtis, C. C.: Initial results from the IMAGE extreme ultraviolet imager, Geophys.

349   Res. Lett., 28, 1439, doi: 10.1029/2001GL012885, 2001.

350   Verbanac, G., Bandic, M., Pierrard, V., and Cho, J.: MLT plasmapause characteristics:

351   Comparison between THEMIS observations and numerical simulations. J. Geophys.

352   Res: Space physics, 123, 2000-2007, doi:10.1002/2017JA024573, 2018.

353   Weimer, D. R.: An improved model of ionospheric electric potentials including

354   substorm perturbations and application to the Geospace Environment Modeling

355   November 24, 1996, event., J. Geophys. Res., 106, 407-416,

356   doi:10.1029/2000JA000604, 2001.

357   Zhang, H., Xu, R. L., Zhao, H., and Shen, C.: The characteristics of the model of

358   Weimer's electric field within the magnetosphere., Chinese J. Geophys. 55, 36-45, doi:

359   10.6038/j.isnn.0001-5733.2012.01.004, 2012.

360   Zhang, H., Xu, R. L., Shen, C., and Zhao, H.: The simulation of the plasmaspheric

361   morphology during a magnetospheric disturbance event, Chin J. Geophys, 56,

362   731-737, doi:10.6038/cjg 20130302, 2013.